

Synthesis of Aluminum Sulfate from Kaolin and Its Thermal Decomposition

Seong S. Park, Hyo K. Kang*, Hong C. Park and Hee C. Park

Dept. of Inorganic Materials Engineering, Pusan National University, Pusan 609-735, Korea
*Kyung Nam Center, Korea Institute of Industry and Technology Information, Chang Won 641-041, Korea

카올린으로부터 알루미늄황산염의 합성 및 열분해

박성수 · 강효경* · 박홍채 · 박희찬

부산대학교 무기재료공학과

*산업기술정보원 경남지역기술센터

(1997년 9월 5일 받음, 1997년 12월 8일 최종수정본 받음.)

초 록 카올린을 용해시킨 황산용액을 에탄올에 주입함으로써 알루미늄황산염의 침전물, $Al_2(SO_4)_3 \cdot 18H_2O$ 을 제조하고, 그것의 열분해거동을 검토하였다. 합성된 고순도의 침전물은 약 $2\mu m$ 크기의 판상형태의 입자들로 구성되어 있었다. 에탄올속으로 카올린을 용해시킨 황산용액의 주입속도를 증가시키에 따라서 생성된 침전물의 결정자 크기는 감소 하였다. 침전물의 탈수 및 탈황산에 대한 겔보기 활성화에너지는 각각 $11.9 kcal mol^{-1}$ 과 $48.2 kcal mol^{-1}$ 이었다.

Abstract Aluminum sulfate, $Al_2(SO_4)_3 \cdot 18H_2O$ was prepared by adding of kaolin-dissolved sulphuric acid into ethanol and its thermal decomposition behavior was discussed. As-synthesized high purity precipitate particles were plate-like shapes of $\sim 2\mu m$ size. With increasing drop rate of leach liquor into ethanol, the crystallite sizes of the precipitate decreased. The apparent activation energies for dehydration and sulfate decomposition of the precipitate were 11.9 and $48.2 kcal mol^{-1}$, respectively.

1. Introduction

The characteristics of ceramic powders are usually affected by many factors such as their chemical compositions, particle sizes and shapes, agglomeration, additives, and impurities. Some of these factors have been investigated¹⁾. Several wet chemical methods have been developed for the preparation of high-purity, homogeneous, and sinterable ceramic powders^{2, 3)}. The simplest method is the precipitation technique. This process consists of four main stages : 1) precipitation of metal cations in the solution, 2) filtering, 3) drying, and 4) thermal decomposition.

Alumina, due to its high melting point ($2050^\circ C$), chemical stability, and optical and electrical properties, is a useful ceramic material. It has been reported⁴⁻⁷⁾ on the preparation of alumina powders by precipitation technique from several precursors and the resulting characteristics have been studied. Generally alumina powders prepared by calcination of aluminum sulfate have high reactivity and sinterability, which are determined by the method of preparation for starting aluminum sulfate^{3, 4, 8, 9)}.

In this work, in order to obtain the useful fundamental data for the preparation of high-performance oxide powders from natural ceramic raw material, we prepared the alumina precursor, aluminum sulfate using Hadong kaolin and investigated its thermal decomposition behavior.

2. Experimental

The synthesis procedure of the aluminum sulphate powders by acid leaching of kaolin is briefly shown in Fig. 1, and described in detail elsewhere¹⁰⁾. Leaching were carried out in a pyrex glass reactor immersed partially in a water bath. Mixing of the solution was done using a stirrer driven by a speed motor. The glass reactor was fitted with a thermometer and a reflex condenser. After calcination at $800^\circ C$ for 3 h, the as-received kaolin was ground to $< 0.074 mm$ in an agate mortar. 600ml of 1.0M sulfuric acid and 18g of kaolin sample were charged into the reactor. The solution was continuously stirred under 450r.p.m at $80^\circ C$ for 3h. After leaching, the glass reactor was cooled to room temperature. Leach residue containing mainly silica was separated by filtering the solution. The filtered

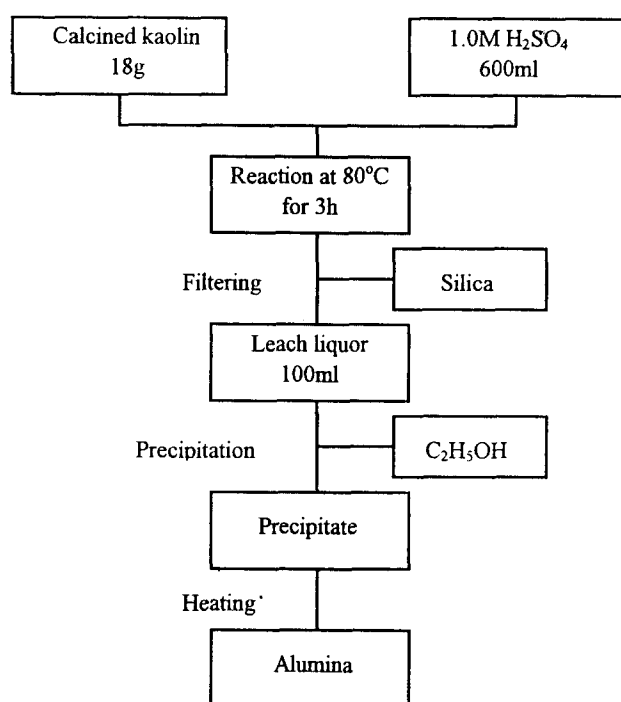


Fig. 1. Experimental flow chart.

leach liquor (200ml) was added with different drop rates (0.5, 1.0, 2.0, 3.0, 4.0, and 5.0ml min⁻¹) into 900ml of stirred ethanol which was used as a precipitating agent. The precipitation occurred just after addition of the leach liquor into the ethanol. The precipitates were dried at 80°C for 24h after washing them again with ethanol.

Crystalline phases were identified by X-ray diffraction (D/Max-2400, Rigaku) with CuK α radiation. Thermal decomposition behaviors of the precipitates were investigated by differential thermal analysis (TG/DTA 2000, Macscience). The microstructures of the precipitates were observed with a scanning electron microscope (JSM-5400, Jeol). Impurities of the precipitates were determined using a plasma spectrometer (SPS-

7700, Seiko).

3. Results and Discussion

As shown in Table 1, XRD data for precipitate prepared from kaolin was comparable with that of Al₂(SO₄)₃·18H₂O (JCPDS No. 26-1010).

Fig. 2 shows DTA and TG curves for a precipitate sample. Thermal analyses were carried out to 1000°C with a heating rate of 10°C min⁻¹. Two endothermic peaks were observed; the first peak at 180°C corresponded to dehydration and the second at 800°C corresponded to desulphurization. Total weight loss due to thermal decomposition was 80 wt%.

As-synthesized precipitate contained <11.4ppm impurities (Table 2). According to the CRC handbook⁽¹⁾, iron sulphate hydrates are absolutely soluble in ethanol. Therefore, the amount of Fe contained in the precipitate was negligible. It is interesting to note that ethanol is a precipitation agent which is used to obtain a

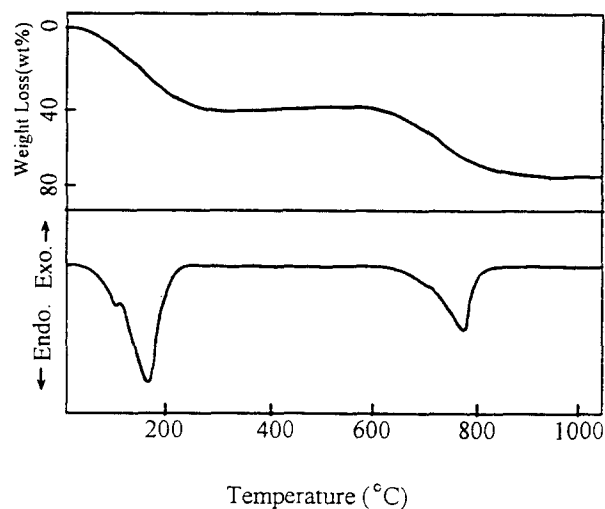


Fig. 2. DTA and TG curves for the precipitate derived from kaolin.

Table 1. XRD data of Al₂(SO₄)₃·18H₂O from both the Joint Committee on Powder Diffraction Standards (JCPDS) and the precipitate derived from kaolin in this study.

| JCPDS (No. 26-1010) | | | Precipitate | |
|---------------------|--------|-----------|-------------|-----------|
| hkl | d(nm) | I / I max | d(nm) | I / I max |
| 020 | 1.350 | 55 | 1.358 | 49 |
| 110 | 0.727 | 22 | 0.718 | 12 |
| 041 | 0.4489 | 100 | 0.449 | 100 |
| $\bar{1}31$ | 0.439 | 80 | 0.411 | 44 |
| 111 | 0.4329 | 75 | 0.4349 | 36 |
| $\bar{1}\bar{3}1$ | 0.3969 | 80 | 0.3913 | 31 |
| 180 | 0.3022 | 35 | 0.3025 | 31 |
| $\bar{2}41$ | 0.2956 | 20 | 0.2976 | 13 |

Table 2. Impurities of the precipitate derived from kaolin.

| Constituent | ppm |
|-------------|-------|
| Fe | 0.683 |
| Na | 7.263 |
| K | 1.747 |
| Mg | 0.533 |
| Ca | 1.162 |



Fig. 3. SEM micrograph of the precipitate derived from kaolin.

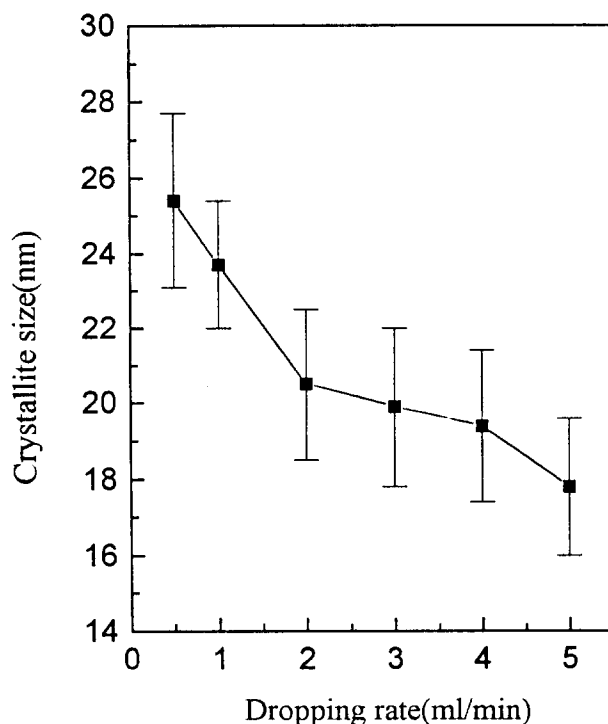


Fig. 4. Crystallite size of the precipitate with drop rate of leach liquor into ethanol.

precipitate with a high purity. The precipitate consisted of plate-like shaped particles of $\sim 2\mu\text{m}$ size, as shown in the SEM micrograph in Fig. 3.

Fig. 4 shows the change of the crystallite sizes of the

precipitate with the different drop rates of leach liquor into ethanol. Crystallite size was determined using the Scherrer formula¹²⁾ with (041) peak in XRD patterns of the precipitate.

The variation of the crystallite size was predicted by the empirical algebraic equation formulated by von Weimarn¹³⁾. Crystallization is divided into two stages ; nucleation (stage I) and growth of nuclei (stage II) with the velocities of each stage represented as

$$V_1 = k(Q-L)/L \quad (1)$$

$$V_2 = DA(C-L)/\delta \quad (2)$$

In addition, the ultimate size of the crystallite (G_m) in number of moles per particle, is given by

$$G_m = K/(Q-L)^n \quad (3)$$

where Q is the instantaneous concentration of the material in solution (metastably) just prior to nucleation, L the equilibrium solubility of bulk solid, D the diffusion constant of the molecules, A the total area of growing crystallites, δ the thickness of a layer around each particle within which the solution is just saturated (concentration L), C the time-dependent solution concentration outside this layer (falling from Q to L with increasing time), and k , K , and n are empirical constants related to the chemical composition of the solid and to the experimental conditions.

The variation of crystallite sizes according to drop rate is estimated mainly in terms of Q and L , although they are of little quantitative value. Large Q and low L values provide a high nucleation rate, as shown in equation (1). If many nuclei form, each nucleus becomes small, as in equation (3). Therefore, an increase in drop rate induces a high solute concentration and formation of many nuclei, resulting in a small crystallite size of the precipitate.

Fig. 5 shows XRD patterns for the precipitate with increasing calcination temperatures up to 1200°C . The as-synthesized precipitate, $\text{Al}_2(\text{SO}_4)_3 \cdot 18\text{H}_2\text{O}$ was finally transformed to $\alpha\text{-Al}_2\text{O}_3$ via $\text{Al}_2(\text{SO}_4)_3$ (600°C) and $\gamma\text{-Al}_2\text{O}_3$ (1000°C).

The results of TG/DTA (Fig. 2) and XRD (Fig. 5) analyses show that the thermal decomposition reactions of aluminum sulfate hydrate can be divided into two stages ; dehydration (equation 4) and desulphurization (equation 5) :



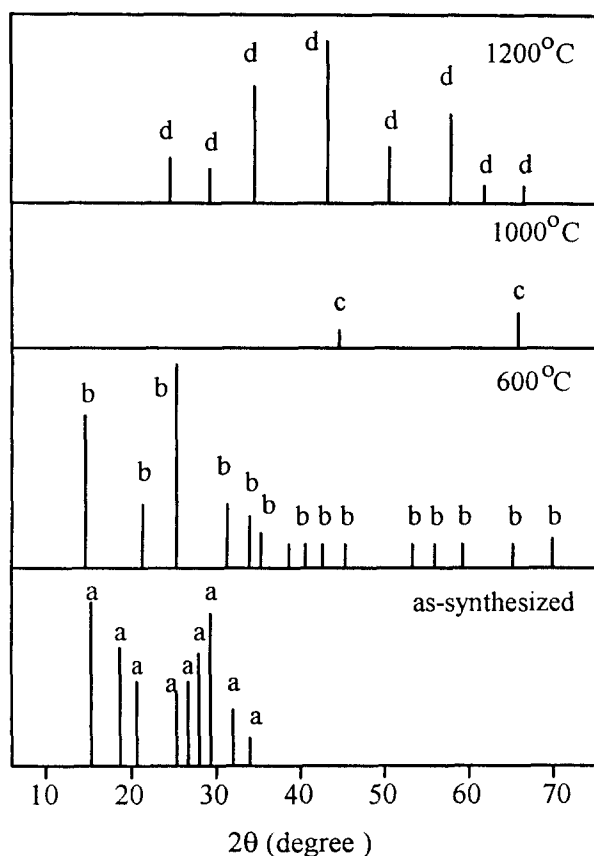


Fig. 5. XRD patterns for the precipitate derived from kaolin, calcined at various temperatures for 2h.
 a : $Al_2(SO_4)_3 \cdot 18H_2O$, b : $Al_2(SO_4)_3$, c : $\gamma-Al_2O_3$, d : $\alpha-Al_2O_3$

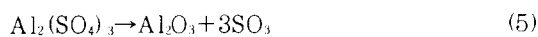


Table 3 shows the DTA peak temperatures for the dehydration and desulphurization stages of the precipitate. With increasing heating rate in the range 5 to 20 °C min⁻¹, peak temperatures moved toward higher: 112 to 150°C for dehydration and 730 to 791°C for desulphurization. Dehydration and desulphurization kinetics were analyzed using Kissinger's method⁽⁴⁾ :

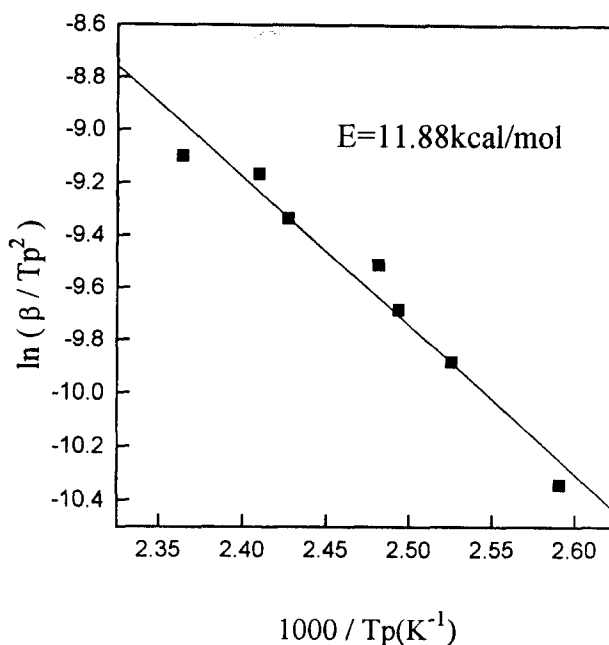


Fig. 6. Kissinger plot for dehydration of the precipitate.

$$\ln \frac{\beta}{T_p^2} = -\frac{E}{RT_p} + \text{constant} \quad (6)$$

where β is the rate of heating, T_p the peak temperature in degrees Kelvin of the endothermic or exothermic reactions, E the activation energy of the process, and R the universal gas constant. The activation energy for the thermal decomposition reaction can be obtained from a plot of $\ln(\beta/T_p^2)$ vs $1/T_p$.

The apparent activation energies for dehydration and desulphurization calculated from the slopes of straight lines were 11.9 (Fig. 6) and 48.2 kcal mol⁻¹ (Fig. 7), respectively. The apparent activation energy for sulfate decomposition of the precipitate synthesized in this study was lower than that (69.3 kcal mol⁻¹) for anhydrous aluminum sulfate crystals⁽¹⁵⁾ obtained from precip-

Table 3. DTA peak temperatures at different heating rates for dehydration and sulphate decomposition of the precipitate derived from kaolin.

| Heating rate, β (°C min ⁻¹) | DTA peak temperature, T_p (K) | |
|---|---------------------------------|------------------------|
| | Dehydration | Sulphate decomposition |
| 5 | 386 | 1003 |
| 8 | 396 | 1022 |
| 10 | 401 | 1031 |
| 12 | 403 | 1038 |
| 15 | 412 | 1043 |
| 18 | 415 | 1055 |
| 20 | 423 | 1064 |

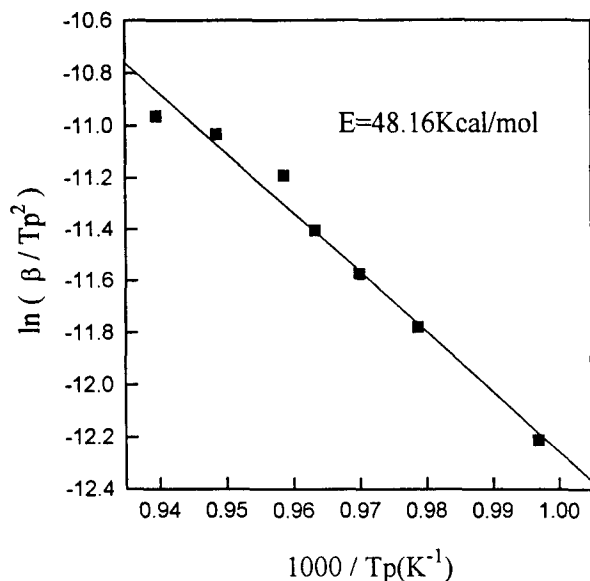


Fig. 7. Kissinger plot for sulfate decomposition of the precipitate.

itation with concentrated sulfuric acid and then calcined at 350°C.

4. Conclusions

High purity hydrated aluminum sulfate containing < 11.4 ppm impurities was prepared by a precipitation technique using Hadong kaolin as a starting raw material. Ethanol was a useful precipitation agent. The crystallite sizes of precipitate were governed by the drop rate of kaolin-dissolved sulphuric acid into ethanol. Thermal decomposition of the precipitate proceeded in two stages ; dehydration at a lower temperature (~140 °C) and desulphurization at a higher temperature (~800°C), with activation energies of 11.9 and 48.2kcal mol⁻¹, respectively. With increasing calcination temperature up to 1200°C, the as-synthesized precipitate, crys-

talline Al₂(SO₄) · 18H₂O transformed to Al₂(SO₄)₃, γ-Al₂O₃, and α-Al₂O₃ in sequence.

References

1. A. Roosen and H. Hausner, *Adv. Ceram. Mat.*, **3**, 31 (1988).
2. J. D. W. Johnson, *J. Am. Ceram. Soc. Bull.*, **60**, 221 (1981).
3. J. E. Blendell, H. K. Bowen, and R. L. Coble, *Am. Ceram. Soc. Bull.*, **63**, 797 (1984).
4. T. Sato, F. Ozawa, and S. Ikoma, *J. Appl. Chem. Biotechnol.*, **28**, 811 (1978).
5. T. V. Mani, P. K. Pillai, A. D. Damodaran, and K. G. K. Warriar, *J. Mat. Lett.*, **19**, 237 (1994).
6. Z. Yu, Q. Zhao, and Q. Zhang, *J. Mat. Sci. Lett.*, **14**, 531 (1995).
7. J. L. Henry and H. J. Kelly, *J. Am. Ceram. Soc.*, **48**, 217 (1965).
8. H. K. Kang, K. H. Kim, and H. C. Park, *J. Mater. Sci. Lett.*, **14**, 1338 (1995).
9. H. K. Varma, T. V. Mani, A. D. Damodaran, and K. G. Warriar, *J. Am. Ceram. Soc.*, **77**, 1597 (1994).
10. H. K. Kang, K. H. Kim, and H. C. Park, *J. Mat. Sci. Lett.*, **14**, 425 (1995).
11. D. R. Lide, *CRC handbook of chemistry and physics*, 74th ed, pp. 4-66, Chemical Rubber company, London, England.
12. B. D. Cullity, *Elements of X-ray Diffraction*, pp. 102, Addison-Wesley, Reading, MA (1978).
13. P. P. Von Weimarn, *Collid Chemistry*, vol 1, pp. 27, ed. by J. Alexander, Chemical Catalog, New York (1926).
14. H. E. Kissinger, *Analy. Chem.*, **29**, 1702 (1957).
15. E. Kato, K. Daimon, and M. Nanbu, *J. Am. Ceram. Soc.*, **64**, 436 (1981).